Chemistry—Methods

Review
doi.org/10.1002/cmtd.202200042

Chemistry Europe
European Chemical
Societies Publishing

www.chemistrymethods.org

Beginner's Guide to Raman Spectroelectrochemistry for Electrocatalysis Study

Weiran Zheng*[a, b]

Chemistry—Methods

Review

doi.org/10.1002/cmtd.202200042

Chemistry Europe
European Chemical
Societies Publishing

The need for continuous observation of electrocatalytic processes under operating conditions has promoted the popularity of in situ techniques coupled with electrochemical tests. In situ Raman spectrometer coupled with electrochemistry (or Raman spectroelectrochemistry) is a powerful tool to provide real-time structural information related to the dynamic electrolyte/electrode interface. To make it more accessible among the electrocatalysis community, we provide an essential experimental guideline of in situ Raman spectroelectrochemistry to beginners. After the necessary background of the technical principle and primary applications, we focus on the experimental considerations, from electrode preparation, cell design, and laser parameters to the electrochemical sequence and data process. The recent efforts to make this technique more affordable are also highlighted. We hope this review can help beginners to understand and use Raman spectroelectrochemistry.

1. Introduction

Electrochemistry has been a much-anticipated research sector in modern chemistry as the foundation of many critical solutions to our generation's energy and environmental-related crises. Typically, most efforts fall into two categories, including electrocatalytic molecule conversion and electrochemical energy conversion. Some specific examples include electrochemical CO_2 reduction, N_2 reduction, biomass conversion, water electrolysis (hydrogen evolution reaction: HER; oxygen evolution reaction OER), rechargeable cells, fuel cells, etc.[1] Multidisciplinary approaches are explored, from material synthesis and electrochemical cell design to reaction optimization and evaluation, aiming to deliver future-proof technologies with superior performance at competitive costs. Yet, apart from rechargeable batteries, most technologies remain immature due to either performance drawbacks or high costs. To address these challenges, researchers need to clarify the electrochemical mechanisms to guide the rational design of both materials and reactions for better efficiency, longer lifetime, and lower price.

Understanding electrochemical processes under operating conditions requires coupling electrochemical cells with characterization methods, and the choice of technique depends on the regions of interest and the desired information.[2–4] For example, surface probe microscopies, such as atomic force microscopy (AFM) and scanning tunneling microscopy (STM), can provide real-time morphological details on the electrode surface;[5–6] X-ray related technologies (X-ray diffraction: XRD; X-ray absorption spectroscopy: XAS; X-ray photoelectron spectroscopy: XPS) can reveal the structure and surface electronic properties;[7–9] mass spectroscopy can detect the electrochemically generated intermediates and products.[10] One family of the in situ technologies with particular interest is spectroelectrochemistry, which combines electrochemical studies with spectroscopic methods, such as UV-vis and infrared.[11–12] The general technical principle involves light being introduced onto the electrode/electrolyte interface to interact with local species, and the photons can be reflected, absorbed, scattered, and emitted. Examining the energy of these photons during electrochemical processes can reveal the dynamic structural details of the interface on a temporal and spatial scale.

Raman spectroelectrochemistry is one of the most popular spectroscopic technologies for electrochemical studies, capable of providing structural analysis of regions from the bulk electrolyte to the diffusion layer in the electrochemical double layer (EDL), and to the surface-adsorbed molecules and electrode material. First demonstrated by M. Fleischmann et al. in 1973,[13] Raman spectroelectrochemistry has been evolving rapidly in pursuit of higher sensitivity, better resolution, and broader application, from both instrumental and methodologic perspectives. Compared to the last century, commercial instruments equipped with high-performance light sources and detectors (e.g., confocal Raman microscopy) are more accessible and user-friendly to researchers who are not Raman experts. As a result, more and more electrochemists can employ powerful Raman spectrometers in their electrochemical research. Specifically, driven by the need to detect weak signals from molecules adsorbed on electrodes, various Raman characterization techniques are invented, such as surface-enhanced Raman spectroscopy (SERS), tip-enhanced Raman spectroscopy (TERS), and shell-isolated nanoparticle-enhanced Raman spectroscopy (SHINERS).

Although its outstanding capability in analyzing electrochemical processes has been demonstrated by many groups, Raman spectroelectrochemistry is not yet widely regarded as a conventional and essential tool for electrocatalysis by many researchers. There are mainly two reasons. First, some researchers from other disciplines are not clear about what information Raman spectroelectrochemistry can provide. Second, some lack experience with experimental setup or access to Raman instruments. In this regard, a beginner's guide to the technique is urgently required for the community. Instead of reviewing the state-of-the-art development of Raman spectroelectrochemistry as readily presented by others, herein, we focus on a rather technical and tutorial review, aiming to address two main questions for beginners: 1) how can Raman spectroelectrochemistry help one's research? 2) how to set up and run a Raman spectroelectrochemistry experiment?

[a] Dr. W. Zheng
Department of Chemistry
Guangdong Technion-Israel Institute of Technology
515063 Shantou (P. R. China)
E-mail: weiran.zheng@gtiit.edu.cn

[b] Dr. W. Zheng
Technion – Israel Institute of Technology
32000 Haifa (Israel)

Chemistry—Methods

Review

doi.org/10.1002/cmtd.202200042

Chemistry Europe

European Chemical
Societies Publishing

2. Technical Principle

Before diving into the instrumental and experimental details, it is essential to understand the principle of Raman spectroscopy. Since any textbook of modern analytical chemistry should have a dedicated section for this technique, we provide a relatively brief introduction here.

Raman spectroscopy relies on the energy exchange between light (photons) and a sample. From an energy level perspective, the incident light can stimulate the transitions of energy levels from the stable ground state to a virtual state (Figure 1A). Such a state is highly unstable and tends to return to the ground state within 10^{-12} s. The relaxation can be accomplished by returning to the same initial ground state with the emission of photons with the same energy as the incident photons (Rayleigh scattering). Meanwhile, since the ground state contains many vibronic sublevels, the virtual state can return to other sublevels, emitting photons with altered energy values (Stokes scattering: to lower energy photons; Anti-Stokes scattering: to higher energy photons). Both Stokes and anti-Stokes scattering are called Raman scattering. When the excitation photon carries energy close to the transition energy between two electronic states of the material, the relaxation occurs firstly from the virtual state to the higher electronic state, followed by a fluorescence process to the lower electronic state. The fluorescence signals contribute to the background of Raman scattering and need to be minimized.[14]

Typically, when the sample is irradiated with light, most photons are scattered without energy change, and only a tiny portion has altered wavelength values after the scattering (usually one in $10^6 \sim 10^8$), indicative of losing or gaining energy. The discrete wavenumber difference between incident light and scattered light is regarded as the Raman shift (Figure 1B). The intensity of the Stokes scattering is typically higher than the anti-Stokes scattering because most molecules at the ambient conditions stay at the ground state.

Examining these values can provide molecular vibrational insights closely related to the sample structure (electronic levels). Especially, when the virtual state is very close to or of the same energy as the stationary electronic states, the sample molecules can interact much more effectively with the incident photons to produce 10^4 to 10^6 times enhancement of Raman signals, known as the Raman resonance effect. Furthermore,

Figure 1. Principle of Raman scattering. A. Energy diagram showing the origin of Rayleigh, Stokes, anti-Stokes, and fluorescence signal after irradiation. B. Scattering spectrum showing the photon energetic difference via anti-Stokes, Rayleigh, and Stokes scattering, inset illustrates the scattering of incident light on a sample surface.

when the sample (mostly molecules) is close to specific surfaces (Ag, Cu, and Au), Raman signals are enhanced up to 10^{11} times, which lays the foundation for the SERS technique.

From the instrumental perspective, a typical Raman spectrometer includes three parts: an excitation source, a sampling chamber, and a photon detector, as shown in Figure 2. The excitation source is usually a high-intensity laser to provide monochromatic photons. The photons are introduced to the sample surface through the lens and splitters in the sampling chamber. Then, the scattered photons are collected and redirected to the detector for energy evaluation.

When coupled with electrochemistry, no special modification of the Raman spectrometer is required, other than the need to be able to fit the in situ electrochemical cells inside the

Dr. Weiran Zheng is an associate professor of chemistry at Guangdong Technion-Israel Institute of Technology (GTIIT). He was a Research Fellow at the Hong Kong Polytechnic University after obtaining his Ph.D. from Wuhan University, China. His research focuses on understanding the activation and deactivation mechanisms of electrocatalysts from an atomic scale. He specializes in operando techniques coupled with electrocatalytic processes, such as spectroelectrochemistry and atomic force microscopy. (team: www.thezhenggroup.com)
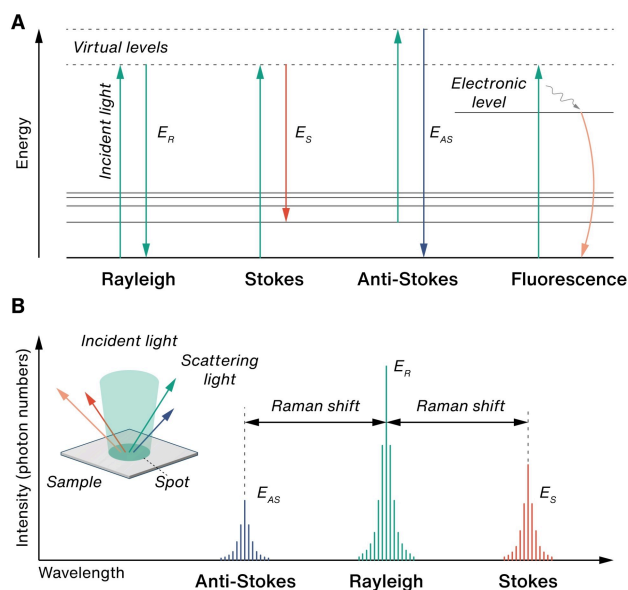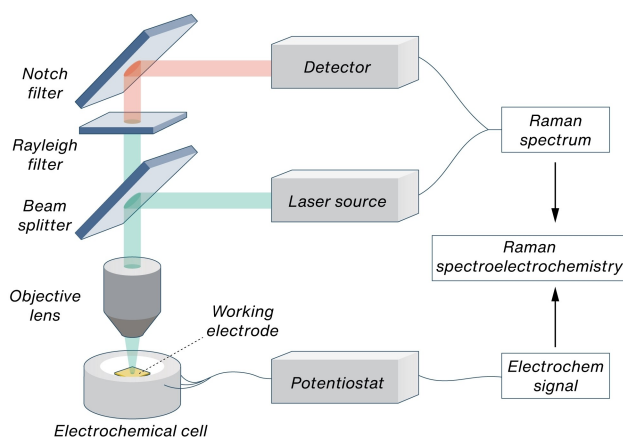
Figure 2. Simplified instrumental illustration of combining Raman spectroscopy with electrochemical analysis as Raman spectroelectrochemistry.

Chemistry—Methods

Review
doi.org/10.1002/cmtd.202200042

Chemistry Europe
European Chemical
Societies Publishing

sampling chamber (Figure 2). As the electrochemical experiment proceeds, Raman signals are continuously collected by focusing the laser on the region of interest. Depending on the study, it can be the electrolyte, surface adsorbed layer, and electrode material. Such flexibility allows the in situ analysis of the electrochemical processes by correlating the structural evolution with electrochemical parameters, such as potential, current, and time.

3. Applications in Electrocatalysis

The capability of Raman spectroelectrochemistry has been widely demonstrated in the thriving fields of electrocatalysis (Figure 3), as summarized in many reviews.[15–17] Here, we provide a general discussion with a glimpse of a few recent examples.

3.1. Structural transition of electrocatalysts

During the electrochemical process, the electrodes (with coated active materials) are subject to rigorous chemical and electrochemical environments. As a result, many unstable materials cannot maintain their structure under operating conditions. Structural transition often occurs before or at the initial stage of electrocatalysis, such as redox, decomposition, surface rearrangement, etc.[18–19] In this regard, the newly formed phases are frequently accounted for in electrocatalysis, acting as the real active sites.[20–21] Understanding the structural transition using in situ techniques is highly desired, and essential to clarify the role of the electrode.

In situ Raman spectroscopy is one of the best tools to track structural evolution and identify active species. It is applicable to many materials, from metal oxides and hydroxides to metal-organic compounds. For example, with the help of in situ spectroelectrochemistry, Yeo and co-workers analyzed the role of CuO and $Cu(OH)_2$ electrocatalysts for alkaline OER, correlating the in situ generated Cu^{III} oxide with their high activity.[22]
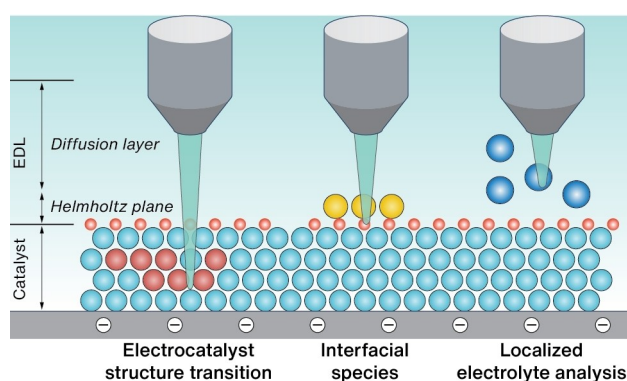

Figure 3. Summary of the main applications of Raman spectroelectrochemistry in electrocatalysis study, from structural transition (left: cyan to red) to interfacial species detection (middle: yellow) and electrolyte analysis (right: blue).

Similarly, Choi et al. tracked the structural transition of NiFe oxide during anodic polarization and identified the formed Ni-OOH as the active species for OER.[23] Recently, we studied the structural evolution of metal-organic framework (MOF) materials under OER conditions using ZIF-67 (zeolitic imidazolate framework-67) as the representative example (Figure 4A).[24] Despite being considered promising electrocatalysts, we demonstrated the completed structural destruction at the early stage of electrochemical studies, forming metal oxyhydroxides as the actual active species. Likewise, real-time monitoring of electrocatalysts using in situ Raman spectroscopy can also provide insights into the catalyst deactivation mechanism. In the study by Koper and co-workers, Pt(111) and Pt(100) oxidation during anodic polarization was elucidated as a sequential two-dimensional Pt oxide to three-dimensional amorphous α-PtO_2 conversion by SHINERS, which may be related to the degradation of Pt-based electrocatalysts in fuel cells.[25]

3.2. Interfacial species on the surface

One main and state-of-the-art application of in situ Raman spectroscopy is the structural analysis of interfacial species on the surface of electrocatalysts. A typical electrocatalytic reaction involves adsorption of reactant(s) on electrode, exchange of electron(s) to generate intermediate(s), and desorption of product(s). The structure of the interfacial species, which often varies with electrochemical parameters and electrode surface properties, determines the reaction efficiency and selectivity to a large extent. Therefore, understanding these molecular structures in the EDL is critical for mechanism analysis. For this purpose, in situ SERS and SHINERS are often employed for their ability to intensify the Raman signal of a thin molecular layer.

A few reactions are extensively studied using in situ Raman spectroscopy, mostly energy conversion processes like oxygen reduction reaction (ORR), water electrolysis, and CO_2 electroreduction reaction (CO2RR).[28] The influence of electrolyte and surface structure on the adsorbates is one common topic. In their study of oxygen reduction reaction (ORR, a critical reaction of fuel cell process) on Pt(*hkl*) surface, Dong et al. presented the Raman spectroscopic evidence showing the reaction intermediates as HO_2^* on Pt(111) (Figure 4B) and OH* on Pt(110) and Pt(100) in acidic conditions, while as O_2^- in alkaline conditions.[26] They also provided a similar analysis on high-index surfaces, such as Pt(211) and Pt(311).[29] Such results explain the morphology-dependent activity of Pt electrocatalysts and their dissolution during fuel cell operation. For CO2RR, copper is known for reducing CO_2 to various products, but clarifying the reaction intermediates to regulate the selectivity remains challenging. Some have been identified with in situ Raman spectroscopy, such as *CO, HCOO*, HOCCO*, and $CH_3CH_2O^*$.[30] Tunning the surface properties of Cu can alter the structure of intermediates and reaction efficiency. Wang and co-workers showed that the rate-determining desorption of HCOO* species on Cu surface could be accelerated by a surface coating of cetyltrimethylammonium bromide.[31]
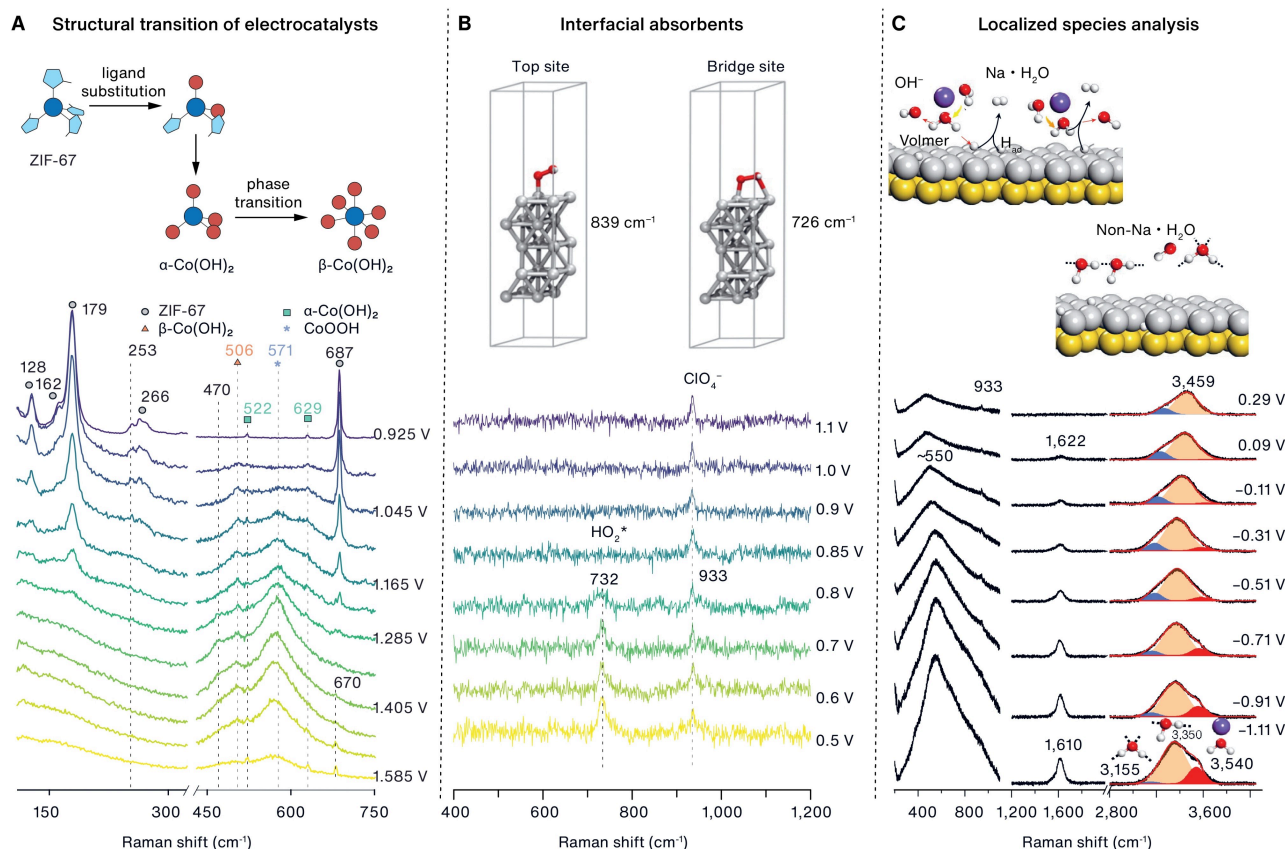
Figure 4. Examples of using in situ Raman spectroscopy for electrocatalytic research: the identified structures (top) were supported by Raman spectra evidence (bottom). A. Structural evolution of ZIF-67 (179 cm^{-1}) with increasing potential, showing the production of α-Co(OH)$_2$ (522 and 629 cm^{-1}), β-Co(OH)$_2$ (506 cm^{-1}), CoOOH (571 cm^{-1}). Reproduced with permission from Ref. [24]. Copyright 2020, American Chemical Society. B. Identification of O—O stretching vibration (732 cm^{-1}) of adsorbed HO$_2$* on Pt(111) during ORR, agreeing with the bridge site. Reproduced with permission from Ref. [26]. Copyright 2018, American Chemical Society. C. Formation of interfacial ordered water structure on Pd(111) surface, indicated by the ~550 cm^{-1} scattering peak. Reproduced with permission from Ref. [27]. Copyright 2021, Springer Nature.

3.3. Localized species analysis in the electrolyte

Further shifting the focus of incident light into the EDL region enables the in situ analysis of the localized electrolyte, specifically the chemical species in the Helmholtz plane and diffusion layer. Such electrolyte is highly sensitive to electrochemical environments and can be easily perturbed by the reaction.

One predominant example is its application in CO2RR. Berlinguette's group recently employed Raman spectroelectrochemistry for local pH determination during CO2RR.[32] By quantifying the HCO$_3^-$ and CO$_3^{2-}$ Raman signals, they were able to calculate the surface pH at various current densities.

Raman spectroscopy is also engaged for real-time water electrolysis studies. Recently, Li and co-workers demonstrated that interfacial water molecules could be nicely probed with the SHINERS technique, outlining the structural transition from a random to an ordered distribution at HER potential to facilitate electron transfer (Figure 4C).[27]

4. Experimental Considerations

Conducting a Raman spectroelectrochemical experiment is not easy, especially for beginners, and a few considerations and troubleshooting must be taken to avoid misleading results. In this section, we provide a detailed experimental guide.

4.1. Working electrode

A typical electrocatalysis study involves three electrodes: the working electrode, the reference electrode, and the counter electrode, while only the electrochemical process on the working electrode is important. The working electrode can be either modified or unmodified, depending on the form of the electrocatalyst. Modified electrodes are prepared by loading the active materials (e.g., nanoparticles) on the surface of electrocatalytically inert electrodes (e.g., glassy carbon electrode, conductive carbon paper) through drop-casting, spin-coating, or chemical growth. Most nanostructured electrocatalysts are characterized in the form of modified electrodes. It should be noted that many inert electrodes can generate Raman signals that complicate the analysis, especially carbon-based ones. For

Chemistry—Methods

Review
doi.org/10.1002/cmtd.202200042

Chemistry Europe
European Chemical
Societies Publishing

example, pristine glassy carbon presents two broad lines at 1340 and 1590 cm^{-1},[33] and carbon paper shows Raman signals at 1351, 1580, and 2703 cm^{-1}.[34] Moreover, further peak position change may occur during the electrochemical analysis. Therefore, thoughtful choice and control experiments under electrochemical conditions are mandatory to ensure the credibility of the spectroelectrochemical data. Unmodified electrodes (e.g., single crystalline metal electrodes) are constructed by electrocatalytically active materials, acting as both the conductor and the electrocatalyst. Different procedures are required for electrode preparation depending on the purpose of in situ Raman analysis and the form of the electrocatalysts.

In principle, if the electrocatalysts can deliver Raman signals, their structural evolution during electrocatalysis can be monitored by in situ Raman spectroscopy. The structural transition in this context is not monolayer formation on the electrocatalyst's surface but an extended phase transition to hundreds of nanometers below the surface that leads to versatile configuration. A few representative examples include metal oxides,[22–23,35–36] metal hydroxides, MXenes,[37] and metal-organic frameworks,[24] while metallic materials do not typically produce Raman signals.

The common causes of the structural changes are: 1. redox reaction: electrochemical reduction or oxidation that promotes the conversion of electrocatalysts to lower or higher oxidation state species (e.g., $Co(OH)_2$ to $CoOOH$ oxidation during OER); 2. phase transition: reaction from chemically unstable phase to stable phase (e.g., α-$Co(OH)_2$ to β-$Co(OH)_2$); 3. decomposition: the destruction of electrochemically unstable materials with weak internal bonding (e.g., ZIF-67).[24] Most modified and unmodified electrodes can be directly characterized without pretreatments. But specific considerations are required. For example, organic binders, such as Nafion 117, are often mixed with electrocatalysts to prepare modified electrodes for higher stability. However, Nafion 117 has various Raman signals (e.g., CF_2 twisting: 307 cm^{-1}; CF_2 symmetric stretch: 725 cm^{-1}; CS stretch: 798 cm^{-1}; SO_3^- symmetric stretch: 1059 cm^{-1}; CC symmetric stretch: 1372 cm^{-1}, etc.) that can sometimes interfere with the sample signal. Therefore, their usage should be reduced or avoided.[38]

Due to the extremely limited molecular amount, SERS is often involved in species analysis on the electrocatalyst surface. Regardless of the working electrode status, a SERS-active substrate is required to produce distinct Raman signals. Typical substrates are rough surfaces of Ag, Cu, and Au, which can significantly enhance the Raman signals of the molecular monolayer (Figure 5A).

The surface can be roughened by many methods, such as chemical etching, electrochemical oxidation-reduction cycling (ORC), physical vapor deposition, etc. For example, chemical etching uses dilute acids (e.g., HNO_3) to corrode the smooth surface and generate nanostructures. The ORC relies on repeated electrochemical oxidation (corrosion) and reduction (deposition) to create nanostructures on the electrode surface. However, the roughening process is random and cannot recreate the identical surface for all tests, posing problems with reproducibility. One way to create a homogenous SERS-active
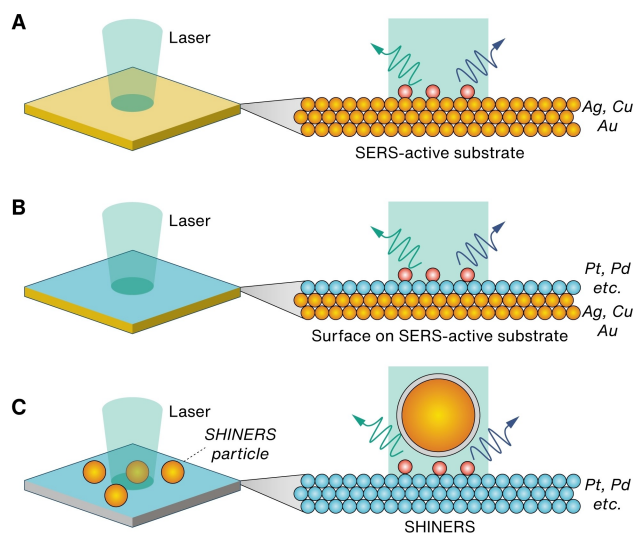
Figure 5. Illustration of working electrodes prepared for enhanced Raman spectroscopy. A. Working electrode as SERS-active substrate; B. Surface coated on SERS-active substrate; C. Surface coated with SHINERS particles.

substrate with controlled roughness is to modify the bare electrode using monodispersed Ag, Cu, and Au nanoparticles, which can be prepared in large volumes with morphological control at a relatively low cost. Tunning the size and shape of the nanoparticles can introduce another degree of freedom for further improvement of the Raman signal intensity. If the subject of the adsorption study is other metals (M), one can coat the SERS-active Au or Ag nanoparticles with a layer of the metal to create a M@Au or M@Ag core-shell nanoparticle as the SERS-active substrate (Figure 5B).[39] But with an ultrathin shell, one may expect the properties of M greatly affected by the underlying Au or Ag. Moreover, as the principle indicates, these roughening methods have changed the surface structures in exchange for a high Raman signal. It is challenging to adopt a similar methodology to flat surfaces, such as single crystalline metal. Tian and co-workers have addressed this problem with the SHINERS technique.[40–41] Instead of roughening the surface, they used the SiO_2@Au (or Ag) core-shell nanoparticles (i.e., shell-isolated nanoparticles, or SHINs) to modify the surface of interest, so the Raman signal from the adsorbates on the surface can be enhanced without directly interacting with the SHINs (Figure 5C). Using such a technique, in principle, electrode surfaces with any material or morphology can be engaged for in situ Raman characterization. The direct analysis of adsorbates on electrocatalysts in the form of nanoparticles is also enabled by SHINERS, known as the SHINERS-satellite technique. The electrocatalyst nanoparticles are decorated on the SiO_2 shell to benefit from the strong electromagnetic field from SHINs, enhancing the Raman signals.[42–43]

4.2. Reference and counter electrodes

Choosing suitable reference and counter electrodes is also critical to ensure reliable electrochemical control. A typical

Chemistry—Methods

Review
doi.org/10.1002/cmtd.202200042

Chemistry Europe
European Chemical
Societies Publishing

reference electrode contains an interface hosting a well-defined half-reaction, whose potential remains constant when a small current pass. However, for some in situ experiments coupled with other techniques (e.g., STM and AFM), quasi-reference electrodes (i.e., pseudo reference electrodes: the electrolyte of the studied reaction is also the electrolyte of the reference electrode) like Ag and Pt wire are used due to the size limitation of the electrochemical cells.[44] Various problems in data analysis are created because the potential of quasi-reference electrodes can drift during electrochemical analysis. Fortunately for Raman spectroelectrochemistry, accurate (or real) reference electrodes (e.g., saturated calomel electrode (SCE), Ag/AgCl electrode, Hg/HgO electrode: electrolyte of the reference electrode is separated from the reaction electrolyte via a liquid junction) can be used thanks to the ample operation space. This advantage guarantees precious control over the potential of the working electrode.[45] However, possible electrolyte leakage through the liquid junction must be noted. For example, conventional SCE and Ag/AgCl electrodes are filled with concentrated KCl solution, which can diffuse into the reaction electrolyte via commonly used porous junctions like ceramic and glass to cause interference. Meanwhile, the changed electrolyte composite of the reference electrodes can lead to potential drifting. Therefore, in most cases, leak-free reference electrodes with a non-porous junction are highly recommended to eliminate possible contaminations from the reference electrodes.

The arrangement of the reference electrode is also important. In an experimental setup, the tip of the reference electrode needs to be placed close to the working electrode to ensure a low iR voltage drop (Figure 6A). One can always obtain and compare the iR value by the built-in electrochemical methods of the potentiostat, such as iR determination and electrochemical impedance spectroscopy (EIS).

Some considerations regarding the counter electrode also need to be taken, including geometry, electrochemical reaction, and possible contamination. Universally, the counter electrode is only used to complete the current circuit and should not impact the kinetics of the electrochemical reaction. Therefore, a larger surface area (or electrochemically active surface area, ECSA, to be more precious) than the working electrode is required, so the ECSA of the counter electrode cannot limit the reaction. Moreover, in the confined Raman spectroelectrochemical cell, the distance between the counter electrode and any selected region on the working electrode should be approximately the same, so the electrical field is evenly distributed. In that case, an annular counter electrode surrounding the working electrode is preferred over the conventional rod shape,[46] but a stacked configuration is also currently popular (Figure 6A).

Meanwhile, the counter electrode should also be inert materials that cannot generate contamination during the experiment. The common choices are Au, Pt, and graphite. However, one may still expect electrochemical reactions on these materials when a large potential or current is applied. For example, during HER testing, the counter electrode acts as the anode, and the corrosion of Pt and the OER are expected.[47] The released species and the gas bubbles will disturb the reaction
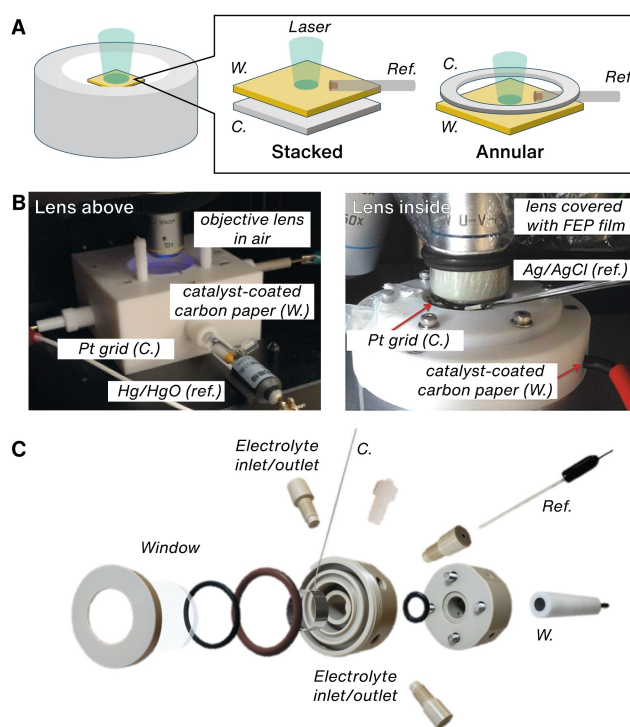

Figure 6. Experimental consideration of electrodes and cells. A. Two common electrode configurations for Raman spectroelectrochemical cell: stacked and annular arrangement. B. Photos of two representative arrangements of the lens with cells: above the electrolyte (left); inside the electrolyte (right). Left: reproduced with permission from Ref. [24]. Copyright 2020, American Chemical Society; Right: reproduced with permission from Ref. [48]. Copyright 2017, Wiley-VCH. C. Schematic drawings of a spectroelectrochemical cell developed by Bott-Neto et al. Reproduced with permission from Ref. [49]. Copyright 2020, Wiley-VCH. *W.*: working electrode; *C.*: counter electrode; *Ref.*: reference electrode.

and obstruct the Raman characterization. The use of H-type cells to separate the counter electrode from the working electrode is required for these cases.

4.3. Electrolyte solution

Before the incident light reaches the electrode surface, it inevitably travels through the electrolyte solution. So the solution must be optically transparent to the incident light and Raman signals, and turbid/colored solutions should be avoided.

Raman scattering contributed by the electrolyte and solvent molecules is often expected and needs to be pre-determined by researchers. In general, water molecules in the aqueous solution have much weaker and simpler Raman signals than the electrolyte and organic solvents. So, the water signals are neglected in most cases. But the common electrolyte species, such as SO_4^{2-} and CO_3^{2-}, can generate Raman scattering signals, and so does organic solvents, such as ethanol. These possible interferents need to be addressed when planning the experiments. As discussed in the following sections, the solution can be either experimental setup or data processing.

Chemistry—Methods

Review
doi.org/10.1002/cmtd.202200042

Chemistry Europe
European Chemical
Societies Publishing

4.4. Electrochemical cell

A customized Raman spectroelectrochemical cell is required for in situ analysis to house the three electrodes discussed above. In general, the design needs to enable the illumination of the working electrode with the incident light and the collection of the scattered photons at a low optical loss by shortening the optical path (typically <1 cm). The configuration of the cell with the Raman spectrometer can be the most challenging part because it can impact the signal significantly. So far, most institutes are equipped with Raman microscopy, a technique combining Raman spectroscopy with conventional optical microscopy, which allows focusing the incident light on a small area to reach a spatial resolution below 1 μm. One improved type called Raman confocal microscopy further enables the depth analysis of samples. In the following context, the discussions are based on this type of equipment.

In a common Raman spectroelectrochemical setup, the objective lens is placed above the electrolyte to irradiate and collect the photons (Figure 6B, left). Besides interfering Raman signal, the electrolyte solution can reduce the incident light intensity and decreases the collection efficiency of the scattered photons. One key consideration for the best outcome is minimizing the electrolyte solution's influence between the lens and the working electrode.

Naturally, a thinner electrolyte layer can deliver a less interfering signal from the electrolyte. However, it should be noted that a larger iR voltage loss is also expected as the surface electrolyte layer gets thinner since fewer electrolyte species are available to conduct electricity. As a result, the electrochemical results of the working electrode in an in situ Raman spectrochemical cell can be different compared to other electrochemical cells, a problematic phenomenon shared by many in situ electrochemical experiments. Therefore, in addition to good Raman signals, researchers need to optimize the thickness of the electrolyte layer for consistent electrochemistry so that all cells (including those for other in situ techniques and conventional electrochemical analysis) deliver the same electrochemical results. In some less rigorous experiments, one may use commercial fluorinated ethylene propylene (FEP) film to wrap the lens so it can be immersed in the electrolyte solution (Figure 6B, right), making the thickness of the electrolyte layer less important.

A few manufacturers currently offer commercially available Raman spectroelectrochemical cells. These cells provide an all-in-one solution to environmentally controlled in situ Raman spectroscopy. Nearly all are constructed with high-performance plastics, such as PTFE (Polytetrafluoroethylene) and PEEK (polyether ether ketone). Regarding chemical resistance, PTFE is virtually inert to most chemicals, while PEEK can be affected by sulphuric acid. The pre-installed reference and counter electrodes are also available for these cells.

As for more demanding experiments, such as those sensitive to oxygen, it is critical to have an environmental control cell. Figure 6C illustrates a sealed cell design by Bott-Neto et al., featuring the inlet and outlet of electrolyte and gas.[49] The electrolyte is no longer exposed to the atmosphere,

and an additional optical window (e.g., sapphire: Al_2O_3; quartz: SiO_2) is required to contain the solution. Consequently, this window material will decrease the intensity of Raman signals and produce interfering signals. In light of this, it is suggested to use thin single crystalline quartz or sapphire as the optical window due to their well-defined Raman signals.[50] Amorphous materials, such as microscope slide glass, should be avoided since they typically produce broad Raman peaks that can conceal minor signals. For less rigorous studies, one can use fused quartz compared to expensive single crystalline materials.

Lastly, we must emphasize that the premise of such customization and optimization of electrochemical components for better Raman signals is the consistency of electrochemical data. Usually, we will expect to couple multiple techniques with the electrochemical reactions for comprehensive understanding, which requires electrochemical cells with different configurations. Therefore, the same electrochemical results need to be reproduced for a meaningful analysis regardless of the cell used.

4.5. Laser parameters

Although no specific instrumental modification is needed for the Raman spectrometer, the parameters must be selected carefully. Those related to the incident light are primarily critical.

In modern Raman spectrometers, the incident light is usually a high-intensity laser in the range from UV to the near-infrared region. The wavelength of the laser, in principle, cannot affect the Raman shifts of the samples but can impact the signal intensity, background fluorescence, and spatial resolution. The most common wavelength includes 532, 632.8, 785, and 1064 nm. Table 1 compares the properties of different wavelengths. The Raman scattering intensity is higher with a shorter wavelength. Therefore, to reach a similar Raman scattering intensity from a 532 nm laser, a higher laser power of a 1064 nm light source or a longer accumulation time is required. Apart from the intensity, suppressing the background fluorescence is also critical to getting distinct Raman signals. A shorter wavelength (e.g., 532 nm) generally will cause the fluorescence emission from samples that overwhelm the weak Raman signals, especially for organic molecules.

Therefore, choosing the most suitable wavelength must balance Raman intensity and background fluorescence. For in situ Raman spectroelectrochemical experiments, the shorter wavelengths (532 and 632.8 nm) are commonly used for the analysis of inorganic materials,[22,51] and 785 nm laser is utilized

Table 1. Comparison of laser wavelengths and properties.

Laser wavelength [nm]	532	632.8 and 785	1064
Excitation efficiency	high	medium	low
Fluorescence	high	medium	low
Spatial resolution	high	medium	low
Heat absorption of sample	low	medium	high
Probing depth	low	medium	high

Chemistry—Methods

Review
doi.org/10.1002/cmtd.202200042

Chemistry Europe
European Chemical
Societies Publishing

when the fluorescence signal needs to be reduced.[24] An example demonstrated by Morávková et al. illustrated the impact of laser wavelength, as shown in Figure 7.[52] When studying the electrochemical oxidation process of polyaniline film, much more details were revealed using 785 nm, while intense fluorescence signals were present with 633 nm.

Spatial resolution is a key parameter when dealing with electrocatalysts, representing the ability to discriminate slight structural differences. In principle, a shorter wavelength laser produces a higher spatial resolution and a low probing depth (resolution of the Z axis). However, when resonance Raman spectroscopy (e.g., SERS) is engaged, laser excitation in resonance with the active materials (e.g., Ag, Cu, Au) should be selected to enable enhanced Raman signals.

Choosing the suitable laser intensity (power) is also essential. During a typical experiment, the laser is focused on a sampling spot with a diameter from a few to 1 μm. A high-intensity laser can heat the irradiation spot and cause sample damage, while a low-intensity laser produces low signal intensity. This is especially important for Raman spectroelectrochemical studies since most in situ generated species (e.g., adsorbates, reaction intermediates, and amorphous structures) are temperature sensitive. Although the sample (working electrode) is being placed within the electrolyte, the instant spike of the local temperature at the sampling spot can still trigger the structural evolution of these species before the heat is conducted. For example, we found that changing the laser power from 1.5 mW to 5.0 mW led to the phase transition of $Co(OH)_2/CoOOH$ to Co_3O_4.[24] In this regard, a good balance is required, which can be achieved only by trial and error. We suggest the researchers start from the lowest energy possible until distinguishable signals evolve. Similar advice also applies to the sampling time (or acquisition time) that prolonged time increases the risk of sample damage. For preliminary verification, researchers may also use integrated optical microscopy to verify the color of the samples before and after analysis. Color change commonly indicates structural evolution, but structural change does not always accompany color difference.
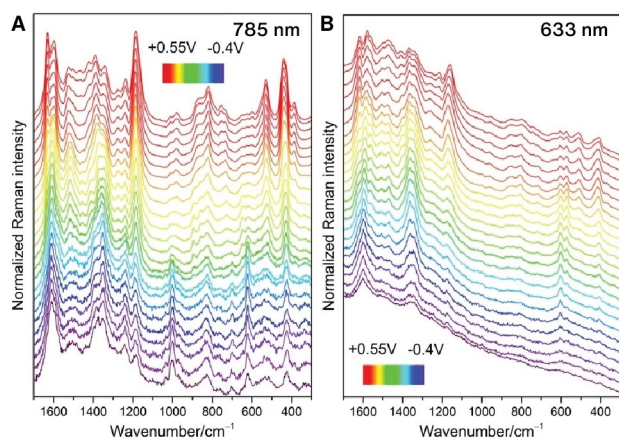
Finally, it must be stressed that the laser needs to be calibrated every time vs. the 520 cm^{-1} peak of silicon standard when either electrode or electrolyte is adjusted. This is to validate the comparison between different experiments or with literature.

4.6. Electrochemical sequence

The key idea of coupling Raman spectroscopy with electrochemistry is to study the interfacial structure at a particular potential. Therefore, during the sampling period (usually a few seconds), the interface needs to remain relatively stable to establish an accurate structure-potential relationship, which limits the selection of electrochemical sequences.

In basic sweep voltammetry (such as linear sweep voltammetry, or LSV), the potential on the working electrode is swept linearly from one value to the other (instrumentally, in the form of a series of small stair steps). As shown in Figure 8 (left), The ever-changing potential of the interface makes it difficult to correlate the collective Raman signals (during T1 and T2) with a specific potential value (V1 and V2). One of the solutions is to decrease the scan rate below 0.5 $mV\,s^{-1}$ so that the potential variation can be neglected. But it extends the experiment time, which may cause further instability issues for the sample.

Another solution is to use the chronoamperometry (or staircase voltammetry) method (Figure 8, right). Unlike the LSV, it engages multiple steps between the initial and final potentials. By defining the step size and time, one can program the working electrode to reach specific potentials and equilibrium for a few seconds before collecting the Raman signals. Because the potential is constant during the Raman sampling, the structure-potential relationship can be established. To enable this, researchers need to synchronize the Raman spectrometer's sampling time, interval, and electrochemical sequence.

Ideally, a shorter sampling time and a smaller interval facilitate less risk of sample damage and deliver a higher time resolution. But in many cases, distinguishable Raman signals evolve only at longer sampling times (typically a few seconds on commercial Raman instruments), limiting the time resolution of Raman spectroscopy. Therefore, to capture fast electro-
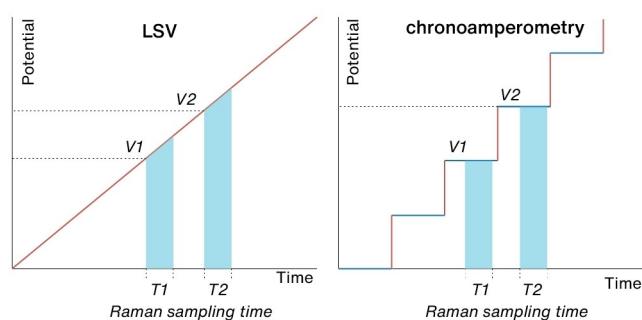
Figure 7. Raman spectra collected during the electrochemical oxidation of polyaniline film from −0.4 V to 0.55 V at different laser wavelengths: A. 785 nm; B. 633 nm. Reproduced with permission from Ref. [52]. Copyright 2017, Wiley-VCH.

Figure 8. Potential sequences of LSV (left) and chronoamperometry (right). The rapid potential change is marked in red, and the equilibrium at constant potential is marked in blue.

Chemistry—Methods

Review
doi.org/10.1002/cmtd.202200042

Chemistry
Europe
European Chemical
Societies Publishing

chemical processes, enhancing the Raman resonance intensity by material design and instrumental optimization to reduce the sampling time is necessary (known as time-resolved resonance Raman (TR³)) to enable spectroelectrochemistry with sampling time down to ms level.[53–55]

4.7. Data process and presentation

After collecting the spectra, researchers are required to process and present the data to support their claims. Apart from the software that comes with the instruments, a few freeware programs are available to view and analyze the raw Raman spectra, such as Spectragryph and Raman Tool Set. The initial steps to prepare the data for further analysis include cosmic spikes removal and wavelength/wavenumber/intensity calibration. Then, baseline correction is required to eliminate the background signals from fluorescence and Rayleigh scattering without harming the sample signals, which remains a challenge in the field.[56] After these steps, researchers will face their biggest problem: band assignment. Most online Raman databases contain only organic fragments (e.g., C—O, C—C, etc.) under ambient conditions, and the Raman response of more extensive material families (e.g., metal oxides, hydroxides, etc.) under electrochemical conditions are largely unknown, especially of those unstable species generated as intermediates during polarization. To resolve the spectra, researchers often dive into publications hoping to find the matching bands. However, people will frequently find contradictory band assignments in the literature due to different electrochemical conditions. Therefore, researchers are suggested to carry out a thorough survey and perform control experiments (e.g., isotope substitution) to justify their assignments. For the bands of the same vibration model, quantitative analysis can be achieved via curve fitting, and the peak area indicates the relative species population.[36] Notably, the quantitative analysis should only be done with spectra collected on the same working electrode within the same experimental sequence using the same peak profile.[57]

The final Raman datasets collected at various potential steps are often enormous, and their analysis can be time-consuming. In many cases, presenting the whole dataset is not necessary, and only the critical spectra need to be identified and shown. Most in situ spectroelectrochemical datasets are offered in two forms: stacked plot and contour plot. Figure 9 shows the examples of each form. The stacked plot shows each spectrum's peak position and intensity but can only contain a limited number of spectra. The contour plot can depict all spectra collected in one figure but is not convenient for analyzing the individual spectrum. A few software programs are available for plotting both types. To list a few, the commercial ones include Originlab and Matlab, and the freeware ones have Veusz scientific plotting package, ggplot2 (with R project), and PRISMA.[58]
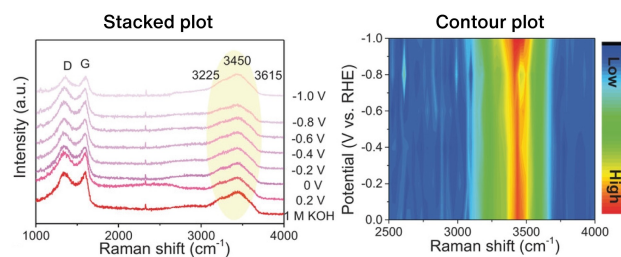

Figure 9. Examples of Raman spectroelectrochemical data presentation: stacked plot (left) and contour plot (right). Reproduced with permission from Ref. [59]. Copyright 2021, Wiley-VCH.

5. Low-cost in situ Raman System

The cost of the in situ Raman spectroelectrochemical system comes from two parts: the electrochemical cell and the Raman spectrometer. Instead of the pricey commercial ones, one can build their system at a much lower cost.

5.1. 3D-printed electrochemical cell

Commercial cells for Raman spectroelectrochemistry are generally priced between 1,000 and 3,000 USD. A cheaper option is to find professionals to produce cell components following published blueprints. Thanks to the emerging 3D printing technology, it is now possible to design and manufacture a customized Raman spectroelectrochemical cell (or any other cells!) at a much lower price (< 20 USD).[60–61] The process involves three steps: 3D design, print and assembly, and test (Figure 10). First, the 3D models of all printable components need to be built with the required features and dimensions, such as the area of the working electrode, the diameter of the reference electrode, optical window size, volume, gas inlet/outlet, liquid inlet/outlet, etc. A few free 3D modeling software are available, like Blender. SketchUp, and Tinkercad. Second, the model files (*.stl* files) are sent to 3D printers for manufacture.
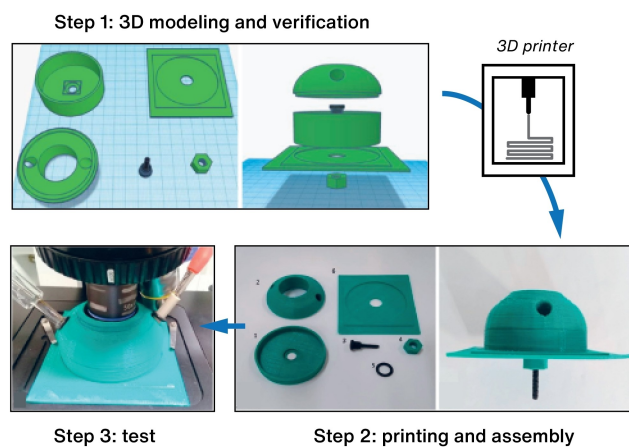

Figure 10. Low-cost and customized Raman spectroelectrochemical cell made by 3D printing. Reproduced with permission from Ref. [60]. Copyright 2019, American Chemical Society.

Chemistry—Methods

Review
doi.org/10.1002/cmtd.202200042

Chemistry Europe
European Chemical
Societies Publishing

We will not repeat the principle of 3D printing here, and the excellent perspective by Tully et al. is recommended.[62] In this process, a few polymer materials (e.g., Nylon, acrylonitrile butadiene styrene: ABS) is available to make the cell. Researchers can choose the polymers with the best chemical resistance to their electrolyte solution. For example, Nylon is resistant to ethanol and ammonia solutions (10%) but not acid solutions. ABS is generally resistant to the aqueous solution of acids but not HNO_3 and concentrated H_2SO_4. In general, PETG (glycol-modified polyethylene terephthalate) is recommended for their excellent chemical resistance. Printing using PTFE and PEEK is also possible with high-temperature printers ($>350\,°C$). Dos Santos et al. used ABS and conductive graphene polylactic acid (PLA) filaments to produce a cell with a cost lower than 2 USD.[60] da Silva Junior et al. created their cell using PETG filament at the cost of 15 USD.[61] The costs are significantly lower than the commercial ones.

5.2. Homemade Raman spectrometer

Despite the long history of Raman spectroscopy, commercial all-in-one Raman spectrometers are generally very expensive ($>90,000$ USD). Instead, one can get modular parts from various suppliers ($<10,000$ USD) to build and configure a Raman spectrometer specifically for electrochemical analysis. Ahn's team demonstrated that using a commercial optical pickup unit, the cost of a functional Raman spectrometer (with performance comparable to commercial ones) can be reduced to below 1,000 USD.[63] An online project named 'OpenRaman' (https://www.open-raman.org) even offers an open-source framework to build individual parts (laser, lens, gating, etc.) into a working Raman spectrometer at a cost down to 3,200 USD. However, careful calibration of the homemade systems is required to ensure a reproducible and accountable result.

6. Conclusion and Outlook

This review provides an introductive guideline for using Raman spectroscopy in electrocatalytic research. Starting from the brief overview of its applications, we discuss in detail the experimental considerations, including working electrode preparation, electrode arrangement, electrolyte, electrochemical cell, laser parameters, electrochemical sequence, and data process/presentation. Furthermore, current opportunities for low-cost Raman spectroelectrochemical systems are introduced, such as 3D-printed cells and homemade Raman spectrometers. We hope this review can help promote the use of in situ Raman spectroscopy in electrocatalytic research by researchers who are either unfamiliar with the technique or have limited resources.

Seeing is believing. In situ techniques, including the Raman spectroelectrochemistry explained in this review, are the premier tools for electrocatalytic mechanism analysis under operating conditions. We expect that more and more reactions will be thoroughly explained as these techniques have been made more available and accessible to a broader community.

Conflict of Interest

The authors declare no conflict of interest.

Data Availability Statement

Data sharing is not applicable to this article as no new data were created or analyzed in this study.

[1] S. M. Jordaan, C. Wang, *Nat. Catal.* **2021**, *4*, 915–920.
[2] A. D. Handoko, F. Wei, Jenndy, B. S. Yeo, Z. W. Seh, *Nat. Catal.* **2018**, *1*, 922–934.
[3] Y. Zhu, J. Wang, H. Chu, Y.-C. Chu, H. M. Chen, *ACS Energy Lett.* **2020**, *5*, 1281–1291.
[4] D. Saurel, A. Pendashteh, M. Jáuregui, M. Reynaud, M. Fehse, M. Galceran, M. Casas-Cabanas, *Chemistry-Methods* **2021**, *1*, 249–260.
[5] W. Zheng, L. Y. S. Lee, *Chem. Asian J.* **2022**, *17*, e202200384.
[6] J. T. Mefford, A. R. Akbashev, M. Kang, C. L. Bentley, W. E. Gent, H. D. Deng, D. H. Alsem, Y. S. Yu, N. J. Salmon, D. A. Shapiro, P. R. Unwin, W. C. Chueh, *Nature* **2021**, *593*, 67–73.
[7] Y. Zhu, H.-C. Chen, C.-S. Hsu, T.-S. Lin, C.-J. Chang, S.-C. Chang, L.-D. Tsai, H. M. Chen, *ACS Energy Lett.* **2019**, *4*, 987–994.
[8] C.-J. Chang, Y. Zhu, J. Wang, H.-C. Chen, C.-W. Tung, Y.-C. Chu, H. M. Chen, *J. Mater. Chem. A* **2020**, *8*, 19079–19112.
[9] D. J. Morris, P. Zhang, *Chemistry-Methods* **2021**, *1*, 162–172.
[10] A. M. Román, J. C. Hasse, J. W. Medlin, A. Holewinski, *ACS Catal.* **2019**, *9*, 10305–10316.
[11] W. Kaim, J. Fiedler, *Chem. Soc. Rev.* **2009**, *38*, 3373–3382.
[12] B. J. Elvers, M. Sawall, E. Oberem, K. Heckenberger, R. Ludwig, K. Neymeyr, C. Schulzke, V. Krewald, C. Fischer, *Chemistry-Methods* **2020**, *1*, 22–35.
[13] M. Fleischmann, P. J. Hendra, A. J. McQuillan, *J. Chem. Soc. Chem. Commun.* **1973**, 80.
[14] E. Smith, G. Dent, *Modern Raman Spectroscopy: A Practical Approach*, 2nd ed., Wiley, **2019**.
[15] K. S. Joya, X. Sala, *Phys. Chem. Chem. Phys.* **2015**, *17*, 21094–21103.
[16] S. Liu, L. D'Amario, S. Jiang, H. Dau, *Curr. Opin. Electrochem.* **2022**, *35*, 101042.
[17] B. Y. Wen, Q. Q. Chen, P. M. Radjenovic, J. C. Dong, Z. Q. Tian, J. F. Li, *Annu. Rev. Phys. Chem.* **2021**, *72*, 331–351.
[18] S. Chen, L. Ma, Z. Huang, G. Liang, C. Zhi, *Cell Rep.* **2022**, *3*, 100729.
[19] L. Liu, X. Li, X. He, J. Yang, N. Liu, *Small* **2022**, *18*, e2104205.
[20] W. Zheng, L. Y. S. Lee, *ACS Energy Lett.* **2021**, *6*, 2838–2843.
[21] B. R. Wygant, K. Kawashima, C. B. Mullins, *ACS Energy Lett.* **2018**, *3*, 2956–2966.
[22] Y. Deng, A. D. Handoko, Y. Du, S. Xi, B. S. Yeo, *ACS Catal.* **2016**, *6*, 2473–2481.
[23] J. Choi, D. Kim, W. Zheng, B. Yan, Y. Li, L. Y. S. Lee, Y. Piao, *Appl. Catal. B* **2021**, *286*, 119857.
[24] W. Zheng, M. Liu, L. Y. S. Lee, *ACS Catal.* **2020**, *10*, 81–92.
[25] Y. F. Huang, P. J. Kooyman, M. T. Koper, *Nat. Commun.* **2016**, *7*, 12440.
[26] J.-C. Dong, X.-G. Zhang, V. Briega-Martos, X. Jin, J. Yang, S. Chen, Z.-L. Yang, D.-Y. Wu, J. M. Feliu, C. T. Williams, Z.-Q. Tian, J.-F. Li, *Nat. Energy* **2018**, *4*, 60–67.

Chemistry—Methods

Review

doi.org/10.1002/cmtd.202200042

Chemistry Europe
European Chemical
Societies Publishing

[27] Y. H. Wang, S. Zheng, W. M. Yang, R. Y. Zhou, Q. F. He, P. Radjenovic, J. C. Dong, S. Li, J. Zheng, Z. L. Yang, G. Attard, F. Pan, Z. Q. Tian, J. F. Li, *Nature* **2021**, *600*, 81–85.

[28] R. Rizo, J. Fernandez-Vidal, L. J. Hardwick, G. A. Attard, F. J. Vidal-Iglesias, V. Climent, E. Herrero, J. M. Feliu, *Nat. Commun.* **2022**, *13*, 2550.

[29] J. C. Dong, M. Su, V. Briega-Martos, L. Li, J. B. Le, P. Radjenovic, X. S. Zhou, J. M. Feliu, Z. Q. Tian, J. F. Li, *J. Am. Chem. Soc.* **2020**, *142*, 715–719.

[30] H. Li, P. Wei, D. Gao, G. Wang, *Curr. Opin. Green Sustain. Chem.* **2022**, *34*, 100589.

[31] Z. Tao, Z. Wu, Y. Wu, H. Wang, *ACS Catal.* **2020**, *10*, 9271–9275.

[32] Z. Zhang, L. Melo, R. P. Jansonius, F. Habibzadeh, E. R. Grant, C. P. Berlinguette, *ACS Energy Lett.* **2020**, *5*, 3101–3107.

[33] M. I. Nathan, J. E. Smith, K. N. Tu, *J. Appl. Phys.* **1974**, *45*, 2370–2370.

[34] A. K. Singh, N. Yasri, K. Karan, E. P. L. Roberts, *ACS Appl. Energ. Mater.* **2019**, *2*, 2324–2336.

[35] A. Y. Faid, A. O. Barnett, F. Seland, S. Sunde, *Electrochim. Acta* **2020**, *361*, 137040.

[36] C. Pasquini, L. D'Amario, I. Zaharieva, H. Dau, *J. Chem. Phys.* **2020**, *152*, 194202.

[37] D. Johnson, H. E. Lai, K. Hansen, P. B. Balbuena, A. Djire, *Nanoscale* **2022**, *14*, 5068–5078.

[38] M. El Boukari, J. L. Bribes, J. Maillols, *J. Raman Spectrosc.* **1990**, *21*, 755–759.

[39] J. F. Li, Y. J. Zhang, S. Y. Ding, R. Panneerselvam, Z. Q. Tian, *Chem. Rev.* **2017**, *117*, 5002–5069.

[40] J. F. Li, Y. F. Huang, Y. Ding, Z. L. Yang, S. B. Li, X. S. Zhou, F. R. Fan, W. Zhang, Z. Y. Zhou, D. Y. Wu, B. Ren, Z. L. Wang, Z. Q. Tian, *Nature* **2010**, *464*, 392–395.

[41] H. Zhang, S. Duan, P. M. Radjenovic, Z. Q. Tian, J. F. Li, *Acc. Chem. Res.* **2020**, *53*, 729–739.

[42] H. Zhang, C. Wang, H. L. Sun, G. Fu, S. Chen, Y. J. Zhang, B. H. Chen, J. R. Anema, Z. L. Yang, J. F. Li, Z. Q. Tian, *Nat. Commun.* **2017**, *8*, 15447.

[43] C. Wang, X. Chen, T. M. Chen, J. Wei, S. N. Qin, J. F. Zheng, H. Zhang, Z. Q. Tian, J. F. Li, *ChemCatChem* **2019**, *12*, 75–79.

[44] A. Auer, J. Kunze-Liebhäuser, *Electrochem. Commun.* **2019**, *98*, 15–18.

[45] R. T. Perera, J. K. Rosenstein, *Sci. Rep.* **2018**, *8*, 1965.

[46] R. A. Timm, E. T. S. G. da Silva, V. C. Bassetto, H. D. Abruna, L. T. Kubota, *Electrochim. Acta* **2017**, *232*, 150–155.

[47] G. Jerkiewicz, *ACS Catal.* **2022**, *12*, 2661–2670.

[48] D. Hollmann, N. Rockstroh, K. Grabow, U. Bentrup, J. Rabeah, M. Polyakov, A. E. Surkus, W. Schuhmann, S. Hoch, A. Bruckner, *ChemElectroChem* **2017**, *4*, 2117–2122.

[49] J. L. Bott-Neto, M. V. F. Rodrigues, M. C. Silva, E. B. Carneiro-Neto, G. Wosiak, J. C. Mauricio, E. C. Pereira, S. J. A. Figueroa, P. S. Fernández, *ChemElectroChem* **2020**, *7*, 4306–4313.

[50] D. Tuschel, *Spectroscopy* **2017**, *32*, 26–33.

[51] Z. M. Wang, W. K. Wang, S. Y. Liu, N. J. Yang, G. H. Zhao, *Electrochem. Commun.* **2021**, *124*, 106928.

[52] Z. Morávková, E. Dmitrieva, *J. Raman Spectrosc.* **2017**, *48*, 1229–1234.

[53] J. V. Perales-Rondon, S. Hernandez, D. Martin-Yerga, P. Fanjul-Bolado, A. Heras, A. Colina, *Electrochim. Acta* **2018**, *282*, 377–383.

[54] S. E. J. Bell, *The Analyst* **1996**, *121*, 107R–120R.

[55] M. Grosserueschkamp, M. G. Friedrich, M. Plum, W. Knoll, R. L. Naumann, *J. Phys. Chem. B* **2009**, *113*, 2492–2497.

[56] S. He, W. Zhang, L. Liu, Y. Huang, J. He, W. Xie, P. Wu, C. Du, *Anal. Methods* **2014**, *6*, 4402–4407.

[57] X. Yuan, R. A. Mayanovic, *Appl. Spectrosc.* **2017**, *71*, 2325–2338.

[58] E. Flores, N. Mozhzhukhina, X. Li, P. Norby, A. Matic, T. Vegge, *Chemistry-Methods* **2022**, *2*, e202100094.

[59] Q. Dai, L. Wang, K. Wang, X. Sang, Z. Li, B. Yang, J. Chen, L. Lei, L. Dai, Y. Hou, *Adv. Funct. Mater.* **2021**, *32*, 2109556.

[60] M. F. Dos Santos, V. Katic, P. L. Dos Santos, B. M. Pires, A. L. B. Formiga, J. A. Bonacin, *Anal. Chem.* **2019**, *91*, 10386–10389.

[61] J. H. da Silva Junior, J. V. de Melo, P. S. Castro, *Mikrochim. Acta* **2021**, *188*, 394.

[62] J. J. Tully, G. N. Meloni, *Anal. Chem.* **2020**, *92*, 14853–14860.

[63] Y. C. Cho, S. I. Ahn, *Sci. Rep.* **2020**, *10*, 11692.